MiR-223 Derived from Mesenchymal Stem Cell Exosomes Alleviates Acute Graft-Versus-Host Disease

Weijiang Liu
Beijing Institute of Radiation Medicine
Na Zhou
Beijing Institute of Radiation Medicine
Peng Wang
Beijing Institute of Radiation Medicine
Yuanlin Liu
Beijjing Institute of Radiation Medicine
Wei Zhang
Beijing Institute of Radiation Medicine
Xue Li
Beijing Institute of Radiation Medicine
Yang Wang
Beijing Institute of Radiation Medicine
Rongxiu Zheng
Tianjin Medical University General Hospital
Yi Zhang (zhangyi612@hotmail.com)
Beijing Institute of Radiation Medicine

Research

Keywords: Mesenchymal stem cells, miR-223, ICAM-1, aGvHD

Posted Date: May 19th, 2020

DOI: https://doi.org/10.21203/rs.3.rs-28347/v1

Abstract

Background Mesenchymal stem cells (MSCs) have been utilized in treating acute graft-versus-host disease (aGvHD) as they show strong immunosuppressive capacity, but the mechanisms are not well defined.

Methods In this study, we demonstrated that microRNA-223 (miR-223) derived from exosomes secreted by human umbilical cord mesenchymal stem cells (huc-MSCs) and murine compact bone mesenchymal stem cells (mb-MSCs) could inhibit aGvHD progression by reducing the migration and homing of donor T cells in aGvHD mice.

Results MiR-223 was one of the conserved microRNAs highly expressed in huc-MSCs exosomes and mMSCs exosomes, which was identified by high-throughput sequencing. MiR-223 derived from MSC exosomes showed enhanced immunosuppressive capacity, as it could inhibit expression of the target gene *ICAM-1* and restrain adhesion and migration of T cells *in vitro*. Moreover, miR-223Agomir was effective in reducing the inflammatory reaction, and declining the donor T cells infiltration into the spleen, liver and intestine in aGvHD mice. Subsequently, it could alleviate aGvHD symptoms. Taken together, the MSC exosome derived miR-223 could attenuate aGvHD in mice through regulating ICAM-1 expression.

Conclusions Our results unveil a new role for MSC exosomes derived miR-223 in the treatment of aGvHD.

Background

Acute graft-versus-host disease (aGvHD) is a severe autoimmune condition caused by immune responses from allogeneic T-cells during hematopoietic stem cell transplantation[1–3]. To date, several studies indicated that MSC treatment of aGVHD by reducing T-cell activation, inducing the regulatory $CD4^+CD25^+$T-cells (Treg cells) and inhibiting the proliferation and activation of antigen-presenting cells (APC) such as dendritic cells [4–6]. Nevertheless, little is known about the regulation of MSCs on these cells.

Mesenchymal stem cells (MSCs), acting as a pleiotropic immune regulator, are reported to suppress immune processes, in which nearly all immune cells including T cells, natural killer (NK) cells, B cells, and dendritic cells (DCs) are affected[4, 6–9]. In the recent years, more attention has paid to potential efficiency of MSCs in aGvHD as they show low toxicity and high expansion *in vitro*[5, 10]. The immunomodulatory effects of MSCs are not always immunosuppressive as it is depending on inflammatory microenvironments[11–13]. The immunoregulatory mechanism of MSCs involves the autocrine or paracrine secretion of factors, chemokines, and exosomes[6, 14]. To date, several studies have shown that exosomes can simulate almost all the biological functions of MSCs[15–18]. Intramembrane DNA, RNA, lipids, proteins, and non-coding RNA of the exosomes participate in the regulation of inflammatory responses[19, 20]. MicroRNAs (miRNAs) play a critical role in the regulation of immune responses. Previous studies demonstrated that several miRNAs (e.g. miR-181c, let-7b, and miR-146b) in the MSC-derived exosomes (MSC-EV) could suppress the inflammatory responses caused by

innate and adaptive immunity[21–23]. Meanwhile, these exosomes can be absorbed by neighboring or distant cells to modulate the function of recipient cells1[16, 19]. These led to a hypothesis that MSCs may secrete exosomal miRNAs, which served as extracellular molecules involving in regulating MSCs immunological functions and potential therapeutic agents for aGvHD.

To explore the therapeutic effects of MSC-EVs derived miRNA on aGvHD, we constructed a miRNAs landscape of human umbilical cord and murine compact bone by high-throughout sequencing, which showed high miR-223 expression. Previous studies indicated miR-223 have effects on inflammation, hematopoietic differentiation and viral infection[24]. In this study, we showed miR-223Agomir could attenuate the aGvHD signs by reducing T cells migration and inflammatory response. These results revealed a novel role of miR-223 in regulating the immunomodulatory properties of MSCs in aGvHD.

Materials And Methods

Reagents

Anti-mouse CD11b (# 12-0112-85), anti-mouse Sca-1 (# 11-5981-82), anti-mouse CD105 (# 12-0900-81), anti-mouse CD34 (# 11-0341-82), anti-mouse CD45 (#14-0451-82), anti-mouse CD31 (# 3-0311-82), anti-human CD73 (# 12-0739-42), anti-human CD34 (# 11-0341-82), anti-human CD105 (# 12-1051-82), anti-human CD45 (# 11-0451-82), anti-human HLA-DR (# 11-9952-42), anti-humanCD166 (# 12-1668-42) were purchased from eBioscience. Mouse anti-ICAM-1 (# sc-8439) was purchased from Santan Cruz biotechnology. Rabbit Anti-TSG101 (# ab125011) and Rabbit Anti-CD63 (# Ab217345) were purchased from Abcam. CellTracker™ CM-DiI (# C7000), cellTracker™ green CMFDA (# C7025), IFN-α Mouse enzyme linked immunosorbent assay (ELISA) Kit (# BMS6027TEN), TNF–α Mouse ELISA Kit (# BMS607HS), IL-17 Mouse ELISA Kit (# BMS6001) were purchased from Invitrogen. Protease/phosphatase Inhibitor Cocktail (# 5872S) was purchased from Cell Signaling. HiFiScript gDNA Removal RT MasterMix (# CW2020) and UltraSYBR One Step RT-qPCR Kit (High ROX, # CW2624) were purchased from CWBIO. ExoEasy Maxi Kit (# 76064) was purchased from QIAGEN. Luciferase®Reporter Assay System (# E1910) was purchased from Promega. CD4 microbeads (# L3T4) were purchased from Miltenyi Biotech. Purified anti-mouse CD3ε (# 145-2C11) and purified anti-mouse IL-4 (# 504101) were purchased from Biolegend, and purified anti-mouse IL-12 (# 505202), purified anti-mouse IFN-γ (# 505701) were purchased from Peprotech. The miRNA agomiR was purchased from RIOBIO. Primers were purchased from Sangon Biotech. HEK 293T (# CRL-1573) and human umbilical vein endothelial cells (HUVECs) (# CRL-1730) were purchased from ATCC. C57BL/6 Mouse Primary Lymphatic Endothelial cells (# C57-6092) were purchased from Cell Biologics.

Mice

Male BALB/c mice served as the recipient mice [8-week-old, specific pathogen free (SPF)]. The donor mice were 6-week-old SPF-grade female C57BL/6j mice (H2kb). Mice were purchased from Beijing Vital River

Laboratory Animal Technology [license SCXK (Beijing) 2016-0001]. All the mice were reared in SPF animal rooms in the Experimental Animal Center at the Beijing Academy of Military Medical Sciences. The recipient mice were fed with sterilized food and water containing gentamicin (320 mg/L) and erythromycin (250 mg/L).

Cell preparation

MSCs, isolated from human umbilical cords and murine compact bone, were cultured in alpha-MEM containing 10% fetal bovine serum (FBS), 100 U/ml penicillin, and 100 mg/ml streptomycin according to the previous description[25, 26]. The cells were cultured to the third passage.

Bone marrow cells and splenocytes were isolated from 6-week-old C57BL/6j mice. Mice were euthanized (carbon dioxide), followed by obtaining the spleen and bone marrow tissues. Erythrocytes were lysed by using erythrocyte lysis buffer. Fresh splenocytes and bone marrow were obtained and washed twice with PBS. These cells were used for transplantation into the irradiated recipient mice.

For the splenocyte staining, the splenocytes for transplantation were labeled with CellTracker™ CM-DiI dye. This was achieved by adding CM-DiI (2 μl) to a splenocyte suspension and incubating at 37 °C in dark for 5 min, followed by incubating at 4 °C in dark for 15 min. PBS was used to remove the unbound dye.

Isolation of exosomes

Serum-free culture medium was used to culture P2 passages huc-MSCs and mb-MSCs. When the cell density of 80% was reached, the supernatant was collected and centrifuged at 700 g for 10 min. The supernatant was collected and centrifuged at 9,000 g at 4 °C for 30 min to remove cell debris. The supernatant was collected, and an exoEasy Maxi kit (Qiagen) was used to isolate the exosomes that were finally resuspended in 100 μL PBS. Then sequencing was performed, which revealed the high expression of miR-223 that was used for the subsequent analysis.

MSC transplantation into C57BL/6j mice

For the experimental group (n = 5), P3 passages MSCs (1×10^6) were injected into mice through the tail vein. An equal volume of PBS was injected into the control group (n = 5). About 48 hrs after treatment, peripheral blood was isolated and centrifuged at 3,000 g for 15 min. The serum was collected to isolate the serum exosomes according to the manufacturer's instructions.

Co-culture of exosomes and HUVECs

HUVECs (2×10^5) were seeded into each well in 6-well plates. The exosomes (2 μg/well) were added to the experimental group, and an equal volume of PBS buffer was added to the control group as previously described[27]. The cells were cultured in RPMI 1640 medium containing 10% FBS for 24 hrs. The supernatant was discarded, and the cells were washed twice with PBS to remove residual exosomes. Finally, 0.25% trypsin was used for digestion, followed by cell collection.

Transient transfection experiment

In total, HUVECs or mouse primary lymphatic endothelial cells (mLECs) were seeded onto 24-well plates (2×10^5/well) and cultured using complete RPMI 1640 medium containing 10% FBS. Upon a cell density of 50–70%, the jetPrime transfection reagent was used to separately transfect miR-223 mimic (100 nM) and negative control. Cells were collected after 48 hrs.

Luciferase

The 293T cells were transfected using Jetprime with pGL3-ICAM-1-3'UTR plasmid, Co-reporter vector pRL-TK (containing renilla) and miR-223 mimic (100 nM). After 48 hrs, the culture supernatant was discarded, and cells were washed once with PBS. The passive lysis buffer from the Dual-Luciferase®Reporter Assay System (Promega) was used to lyse cells, and luciferase activity was measured according to the manufacturer's instructions.

Th1 cell differentiation *in vitro*

$CD4^+$ Th1 differentiation was induced according to the previous study[28]. Briefly, mouse spleen was homogenized followed by filtering through a filter (mesh, 40 μm). Erythrocytes were lysed by using erythrocyte lysis buffer. CD4 (L3T4) microbeads were used to isolate CD4 T-cells, which were then cultured in a 24-well plate coated with anti-CD3ε (3 μg/ml) and anti-CD28 (5 μg/ml). The culture medium contained IFN-γ (20 ng/ml), IL-12 (5 ng/ml), and anti-IL4 (5 μg/ml). Upon cell culture for 3–5 days, flow cytometry was used to measure the expression of IFN-γ and IL-4.

Th1 cells staining

The cells were resuspended gently in CellTracker™ (1:1000, Invitrogen) staining solution. The mixture was incubated at 37 °C for 30 min followed by centrifugation to remove the CellTracker™ Working Solution. The stained cells resuspended with culture media were used for the following assays.

In vitro cell crawling assays

Cultured C57BL/6 mLECs were seeded into coated channeled chamber slides (μ-Slide VI$^{0.4}$, #1709291, IBIDI). Monolayers were transfected with miR-223 mimic and normal control until 24 hrs, and then stained Th1 cells (3×10^4) were added. About 20 min later, chambers were rinsed twice to remove non-adherent Th1 cells. After a further 10 min equilibration at 37 °C, time-lapse imaging was performed on Operetta CLS™ (PerkinElmer Operetta CLS). The images were analyzed using Operetta primarily software.

In vitro transmigration assay

Transferred miR-223 mimic and negative control to mLECs until 24 hrs were seeded onto the upper side of coated Transwell membrane inserts with a pore size of 5 μm (#PIMP12R48, Millipore), followed by culturing until confluence. On the day of the assay, stained Th1 cells (5×10^4) were added in the upper well of the Transwell insert. After 4 hrs, the medium in the bottom well was collected and the number of Th1 cells was quantified by cell counter (Luna).

In vitro adhesion assay

The miR-223 mimic and normal control were transferred to mLECs for 24 hrs, followed by seeding onto a coated 96-well clear bottom (Corning Costar®). Then *in vitro* generated Th1 cells (1×10^4) were added to the mLECs. About 45 min later, non-adherent cells were collected and the number of Th1 cells was measured by cell counter.

Construction of mouse aGvHD model

BALB/C mice (8-week-old) were irradiated with a single dose of 800 cGy total body irradiation (TBI, Co60γ source). The aGvHD model mice were infused with nucleated bone marrow cells (1×10^7) and splenocytes (1×10^7) isolated from C57BL/6 mice (6-week-old) through tail vein injection. After 24 hrs of irradiation, MSCs (P3, 5×10^5/mouse), chemically synthesized miR-223Agomir and micrON^{TM}Ago NControl#22 were used to treat aGvHD.

The miR-223Agomir and micrON^{TM}Ago NControl#22 served as the negative control were centrifuged transiently to achieve miRNA powder aggregation at the bottom of the centrifuge tube. Subsequently, PBS buffer (1 ml) was added to dissolve the powder until a concentration of 50 mol/L, and was administered to recipient mice 1 day before irradiation, as well as 1, 4, and 7 days after irradiation by tail vein injection (10 nmol/mouse).

Western blot

RIPA lysis buffer containing protease inhibitors/phosphatase inhibitors were added to cell pellets (or exosomes) and incubated at 4 °C for 30 min for lysis. Proteins were subject to SDS-PAGE. Next, proteins were transferred onto a PVDF membrane at a constant current of 200 mA for 120 min. The membranes were blocked with 5% skimmed milk-TBST for 1 hr, and CD63, TSG101, and then ICAM-1 antibodies were added. The membranes were incubated overnight at 4 °C. The next day, the membranes were washed with TBST thrice for 10 min. HRP-labeled secondary antibodies were added, and the membranes were incubated at room temperature for 1 hr. Subsequently, the membranes were washed with TBST thrice for 10 min each before imaging.

ELISA

Serum IFN-γ, TNF–α and IL-17 were measured using a commercially available ELISA kit (Invitrogen, USA). All protocols were conducted according to the manufacturer's instructions.

Quantitative qPCR

Total RNA was extracted from exosomes and cells using Trizol reagent. The cDNA synthesis was conducted using the commercial reverse transcription kit (CWBIO). The stem-loop method was used for reverse transcription of miRNA. qPCR was carried out using the UltraSYBR One-Step Kit was according to the manufacturer's instructions. PCR amplification was conducted on the 7500 Real-Time system with GAPDH serving as a reference gene. The specific primers were listed in Table 1.

Table 1
Primer sequence

Gene	Primer sequence (5'-3')
miR-223 Forward	ACACTCCAGCTGGGTGTCAGTTTGTCAA
miR-223 Reverse	CTCAACTGGTGTCGTGGAGTCGGCAATTCAGTTGAGTGGGGTAT
snoRNA202 Forward	ACACTCCAGCTGGGGCTGTACTGACTTGATG
snoRNA202 Reverse	CTCAACTGGTGTCGTGGAGTCGGCAATTCAGTTGAGCATCAGAT
URP	TGGTGTCGTGGAGTCG
human ICAM Forward	ACCATCTACAGCTTTCCGG
human ICAM Reverse	ACACTTCACTGTCACCTCG
mouse GAPDH Forward	ACTCTTCCACCTTCGATGC
mouse GAPDH reverse	CCGTATTCATTGTCATACCAGG
human GAPDH Forward	TCAAGATCATCAGCAATGCC
human GAPDH Reverse	CGATACCAAAGTTGTCATGGA

Statistical analysis

Data were presented as mean ± standard error of mean. When comparing two groups with a sample size of ≥ 3, an unpaired two-tailed Student's t-test was used. Mann–Whitney nonparametric tests were used to compare two independent groups with a sample size of ≥ 3. When data were paired and samples size was ≥ 3, Wilcoxon matched-pairs tests were used. One-way ANOVA were used to compensate for multiple testing procedures. A value of $P < 0.05$ was considered to be statistically significant.

Results

1. Isolation and definition of exosomes from human and murine MSCs

We first isolated and identified MSCs from human umbilical cord according to previous method. Human umbilical cord nucleated cells separated by density gradient displayed fibroblast-like morphology (Fig. 1a). As shown in Fig. 1b, adipogenic differentiation of adherent cells was indicated by accumulation of oil-red-O staining lipid-rich vesicles. In the osteogenic cultures system, the adherent cells displayed strong alkaline phosphatase activity. These results confirmed the multipotency of MSCs. The culture-expanded adherent cells were positive for CD73, CD90 and CD105, and were negative for CD14, CD34, and CD45 (Fig. 1c). All results presented herein indicated that the adherent cells isolated from human umbilical cord were MSCs. Moreover, the characteristics of murine bone derived MSCs (mb-MSCs) were similar to that of human umbilical cord derived MSCs (data not shown).

As MSC-EVs showed similar biological function with the MSCs, we then identified exosomes derived from huc-MSC. Electron microscopy (Fig. 1d) and NanoSight analysis (Fig. 1f) revealed that particles isolated by ultracentrifugation contain abundant hucMSCs-derived EVs with a diameter of 30–100 nm. Expression of exosome-specific markers (i.e. TSG101 and CD63) was detected in these EVs (Fig. 1e). In addition, expression of other exosome-associated protein markers (i.e. CD81 and CD63) was positive by flow cytometry (Fig. 1g). Furthermore, the characteristics of murine MSCs derived from exosome were similar with huc-MSC derived exosomes (data not shown).

2. MSC-EV highly expressed conserved miR-223

To explore the miRNA expression spectrum of murine bone MSC derived exosomes (mb-MSCs-EVs) and human umbilical cord MSC derived exosomes (huc-MSCs-EVs), high-throughput sequencing was used to identify miRNAs of huc-MSCs-EVs and mb-MSCs-EVs. High expression of miR-223 in huc-MSCs-EVs and mb-MSCs-EVs was detected by qPCR supporting the sequencing results (Fig. 2a and 2b). Furthermore, we tested whether MSCs could normally secrete EVs containing functional miR-223 *in vivo* (Fig. 2a). MSC (1×10^6/dose) was injected into C57BL/6j mice (Fig. 2c). After 48 hrs, the serum-derived exosome was isolated, and Western blot analysis of serum exosome-specific markers TSG101 and CD63 was positive

(Fig. 2d). The particles containing mb-MSCs secreted exosomes were observed under an electron microscopy (Fig. 2e). In addition, qPCR analysis showed high expression of miR-223 in these mb-MSCs EVs. Overall, these data showed that MSCs secreted miR-223-containing EVs *in vivo* (Fig. 2f).

3. MSC-EV derived miR-223 inhibited the expression of the target gene *ICAM-1*

Bioinformatic analysis was used to assess the mechanism of MSC-EV derived miR-223 in immunoregulatory function of MSCs *in vitro*, which indicated that it regulated the expression 3'UTR of ICAM-1 (Fig. 3a). Then, we simultaneously transfected ICAM-1-3UTR luciferase reporters and miR-223 mimic into HEK 293 cells. MiR-223 mimic transfection could significantly reduce luciferase activity (Firefly/Renilla) in HEK293T cells ($P < 0.05$, Fig. 3a and 3b).

To further determine the regulatory effects of miR-223 on *ICAM-1*, we transfected miR-223 mimic into HUVECs. qPCR and Western blot analysis indicated significant down-regulation in ICAM-1 mRNA and protein, respectively (Fig. 3c-3e). MSC-EVs (2 μg) were co-cultured with HUVECs for 24 hrs to verify whether exosomes could transport miR-223 into the target cells, which then inhibited target gene expression. These showed that endogenous miR-223 expression was up-regulated in HUVECs, and ICAM-1 protein expression was down-regulated (Fig. 3f and 3 g).

4. MiR-223 restrained T-cell adhesion and migration

Several studies indicated that ICAM-1 in the vascular endothelium was associated with T-cell migration, and ICAM-1 expression was up-regulated in lymphatic vessels and blood vessels in an inflammatory microenvironment, which promoted T-cell migration and inflammatory responses. Based on the inhibition of ICAM expression mediated by miR-223, we further evaluated whether miR-223 could affect T cell migration. After using Th1 induction, the proportion of CD4 cells differentiated into Th1 cells was up to 68.2% (Fig. 4a). The green CellTracker™ labeled Th1 cells were co-cultured with mLEC transfected miR-223 mimics (100 nM) or normal control for 45 min. The results of fluorescence microscope showed that the average numbers of green CellTracker™ adherent cells in transfected miR-223 group showed significant decrease ($P < 0.001$, Fig. 4b and 4c). Concomitantly, the crawling experiment results showed that miR-223 significantly inhibited the migration speed and distance of T cells compared with the negative control group ($P < 0.01$, $P < 0.5$; Fig. 4d and Supplementary video 1 and 2). Moreover, we assessed whether miR-223 could regulate ICAM-1 to change Th1 extravasation. Th1 cells stained with green CellTracker™ were co-cultured with mLEC transfected miR-223 mimics or NC in transwell system for 4 hrs. The number of Th1 cells in the miR-223 group was significantly lower than that of the negative control group ($P < 0.01$, Fig. 4e). These results suggested that miR-223 could restrain Th1 migration and adhesion through ICAM-1.

5. MiR-223 infusion remarkably inhibited the pathogenesis of aGvHD in mice

We further investigated whether miR-223 could inhibit T migration to relieve aGvHD signs. Our data showed that miR-223Agomir contributed to the general growth of aGvHD mice and reduced mortality between days 5 and 17 (Fig. 5a). On day 7 and day 14, the aGvHD presentation scores of mice from the miR-223Agomir group were lower than negative control group and aGvHD group (Fig. 5b). These data proved that miR-223 could reduce aGvHD presentation in mice.

Then we investigated the therapeutic effects of miR-223 on organs and tissues in aGvHD mice using hematoxylin-eosin staining to determine the pathological changes and infiltration of inflammatory cells in spleen, liver, and intestine. After miR-223Agomir treatment, injuries in the spleen, liver and intestines damage were attenuated. The tissue structure remained relatively intact, and the inflammatory cell infiltration showed decline (Fig. 5c). The inflammatory improvement in aGvHD mice caused by miR-223 was further assessed by measuring the expression of proinflammatory factors in serum. Compared with that of the aGvHD group or negative control group, the proinflammatory factors (e.g. IFN-γ, IL-17a, and TNF-α) showed significant decline after miR-223Agomir treatment (Fig. 5d). In total, miR-223 led to attenuation of pathological damage in tissues, and reduce of proinflammatory factor expression in aGvHD mice.

6. MiR-223 reduced migration of donor T cells to recipient spleens

The pathogenesis and progression of aGvHD were considered to be associated with activation and subsequent expansion of donor T cells in recipient secondary lymphoid organs (SLOs). These cells then migrated to peripheral target organs to cause tissue damage by cell mediated cytotoxicity. Flow cytometry results showed that the percentage of splenic $H2kb^+$ CD4 T cell and $H2kb^+$ CD8 T cell was lower in the miR-223 infusion recipient mice compared with that of the aGvHD mice and negative control group (Fig. 6a). The average number of $H2kb^+$ CD4 and $H2kb^+$ CD8 cells showed significant decrease in miR-223 group, which was similar to that of the MSC group (Fig. 6b). These data further implicated the role of miR-223 in MSC-mediated immunosuppression *in vivo*. The effects of miR-223 on MSC were likely to be associated with reducing migration of donor T cells to recipient mice.

7. MiR-223 reduced donor T cell homing to recipient tissues and organs

To further determine the roles of miR-223 in modulating the allogeneic T cell homing, we transplanted CM-dil-labeled splenocytes and bone marrow cells into aGvHD mice. Three days after transplantation, we observed red CM-dil-labeled splenocytes in the spleens, livers, and intestines of each group by

fluorescence microscope. The number of red splenocytes in the negative control and aGvHD group showed significant increase compared with that of the miR-223 group ($P < 0.01$, $P < 0.001$; Fig. 7). These suggested that miR-223 inhibited allogeneic T cell infiltration into the tissues and organs of recipient mice.

Discussion

MSCs are considered as a promising candidate for stem cell therapy for its immunosuppressive properties[6]. Previous studies demonstrated that MSCs had different immunosuppressive functions in different inflammatory microenvironment, depending on the type and concentration of inflammatory factors causing different efficacies for aGvHD[4–6]. Our study showed that MSC-EVs-derived miR-223 attenuated the progression in the mice aGvHD model. MiR-223 treatment had effects on pathological lesions. Meanwhile, it could reduce the donor T cells migration and homing *in vivo*. *In vitro* experiments showed that treatment with MSC-EVs-derived miR-223 directly caused reduction in the adhesion and migration of T cells by inhibiting ICAM-1 expression. These studies suggested that MSC-EVs-miRNAs present similar immunoregulation function to MSCs, which can directly affect the progression of aGvHD.

Some investigations highlighted that the migration of the effector T cells to the target tissues was crucial for the pathogenesis of aGvHD[29, 30]. Nowadays, MSCs have been employed as efficient treatment options for aGvHD. However, MSCs used for aGvHD treatment are mainly administered through intravenous transplantation, which may result in a possibility of remaining in the blood-rich tissues (e.g. liver, lung, and spleen)[2, 5]. Therefore, methods for enhancing homing to the target organ and anti-inflammatory effects of MSCs are urgently needed to improve their clinical efficacy. Accumulating evidence indicated that MSCs could secret exosome, including cytokines, chemokines, and microRNAs in exosome[17, 18]. MSC-EVs showed regulatory effects on peripheral blood monocytes, T cells, B cells, and NK cells[17, 31]. Meanwhile, the effects were depending on the number of exosomes absorbed by T cells[31]. Also, miRNA had been previously reported to be closely involved in immunosuppression by MSC-EV[14, 32]. These experiments demonstrated that MSC-EVs derived miRNA could exert the immunological effects in the therapy. However, elucidation of the molecular mechanisms of MSC-EV derived miRNAs action in aGvHD is pending. Although miRNAs could affect T cells activation and modulate regulatory T cells to ameliorate aGvHD, their roles in the migration of donor T cells infiltration in recipient organs are not clear[33]. In this study, we first reported that MSC EVs-derived miRNA expression spectrum from mb-MSCs and hu-MSCs using high-throughput sequencing. According to the miRNA profile of MSC-EVs, we found that miR-223 was highly expressed and relatively conserved in mb-MSC-EVs and huc-MSC-EVs. Furthermore, the MSCs were transplanted into the C57BL/6j mice, and the serum miR-223 expression showed increase. Here, our data revealed that exosomal miR-223 secreted by MSCs *in vivo* may involve in various physiological activities.

Previous evidence demonstrated that MSCs triggered decline of donor T cells transplanted to the spleen of aGvHD model[34]. However, the specific mechanisms are not well defined. Here, we found that *ICAM-1* was one of the target genes of miR-223, which was identified through a dual-luciferase reporter gene

assay. ICAM-1 could interact with lymphocyte function-associated antigen 1 (LFA-1) to mediate lymphocyte migration, membrane penetration, and activation[35]. Thus, we further showed that miR-223 inhibited ICAM-1 expression on HUVECs and lymphatic endothelial cells, which decreased the T cell migration, the penetration of vascular barriers, and adhesion to lymphatic vessels.

To determine whether the effects of miR-223 on T cells were beneficial to aGvHD treatment, we established the mouse aGvHD model. Then the model was treated with miR-223Agomir after bone marrow transplantation, which showed that miR-223 improved the general growth status in aGvHD mice and simultaneously alleviated lymphocyte infiltration and destruction of the liver, lungs, and other tissues. *In vivo* donor lymphocyte homing results were similar to *in vitro* experiments. Specifically, the donor T cell migration to the spleen, liver, intestine, and lungs in the miR-223 group was lower than that in the other groups. In addition, the effects of miR-223 on T cells also alleviated aGvHD inflammation as the expression of serum IFN-γ, TNF-α, and IL-17 showed significant reduction.

Unlike the previous studies, our study focused on the homing of donor T cells to target tissues. Our data showed that pathological inflammatory responses may contribute to the pathogenesis of aGvHD. Normally, aGvHD occurred upon migration of donor lymphocytes to tissues and organs in the recipient, such as livers, intestine and spleen, which then disrupted the normal function of these organs. lymphocytes may migrate to secondary lymphoid organs for further maturation and activation, which then led to secretion of proinflammatory factors causing subsequent an inflammatory storm and tissue damages. This inflammatory infiltration and destruction thereby induce aGvHD, leading to transplant failure and even death[2, 36].

There are some limitations in this study. We only focused on the fact that miR-223 attenuated the mice aGvHD signs as it could modulate migration of T cells and reduced inflammatory response. However, little is known about the other potential mechanisms underlying miR-223 in aGvHD.

Conclusions

In summary, we found that miR-223 generated by MSC-EVs showed similar biological function with the MSCs. MiR-223 infusion remarkably inhibited the progression of aGvHD in mice. MiR-223 restrained T-cell adhesion and migration via inhibiting the expression of ICAM-1 on both lymphatic and vascular endothelial cells *in vitro*. Meanwhile, it reduced infiltration by donor lymphocytes on organs and tissues, and alleviated inflammation in aGvHD mice. On this basis, we concluded that miR-223 from MSCs derived exosomes alleviated aGvHD occurrence, which would be promising in treating aGvHD. Moreover, little is known about the mechanisms underlying MSC-EVs derived miRNA-mediated suppression of aGvHD. Our studies demonstrated that MSC-EVs derived miR-223 reduced the progression of aGvHD through regulating ICAM-1 expression. Additional studies are necessary to obtain profound understanding on this phenomenon and promote its clinical utilization.

Abbreviations

MSCs: Mesenchymal stem cells

aGvHD: acute graft versus host disease

miRNA: micoRNA

MSC-EV: mesenchymal stem cell derived exosomes

HUVECs: human umbilical vein endothelial cells

mLECs: mouse primary lymphatic endothelial cells

Declarations

Ethical approval and consent to participate

The study protocols were approved by the Ethical Committee of Beijing Institute of Radiation Medicine.

Consent for publication

Not applicable.

Availability of supporting data

The datasets used and/or analyzed during the current study are available from the corresponding author on reasonable request.

Competing interests

The authors declare that they have no competing interests.

Funds

This work was supported by grant from National Key Research and Development Program of China (No. 2016YFC1000305). Tianjin Natural Science Foundation (No. 17JCZDJC36400); Key Research Project of Tianjin Municipal Commission of Health (No. 16KG123); Science and Technology Popularization Project of Tianjin Science and Technology Bureau (No. 18KPHDSF00140).

Author’s contributions

Weijiang Liu: Conception and design, performed research, analyzed data, prepared figures and wrote the paper. Na Zhou: performed research, analyzed data, prepared figures. Peng Wang, Yuanlin Liu, Wei Zhang: performed research, analyzed data. Xue Li, Yang Wang: performed research. Rongxiu Zheng: designed research, analyzed data, prepared figures and wrote the paper. Yi Zhang: designed research, analyzed data, prepared figures, wrote the paper, administrative support and final approval of manuscript. All authors read and approved the final manuscript

Acknowledgements

Not applicable.

References

1. Zeiser R, Blazar BR. Acute Graft-versus-Host Disease. N Engl J Med. 2018; 378:586.
2. Ferrara JL, Levine JE, Reddy P, Holler E. Graft-versus-host disease. Lancet. 2009; 373:1550-1561.
3. Zeiser R. Activation of Innate Immunity in Graft-versus-Host Disease: Implications for Novel Targets? Oncol Res Treat. 2015; 38:239-243.
4. Wang Y, Chen X, Cao W, Shi Y. Plasticity of mesenchymal stem cells in immunomodulation: pathological and therapeutic implications. Nat Immunol. 2014; 15:1009-1016.
5. Zhao L, Chen S, Yang P, Cao H, Li L. The role of mesenchymal stem cells in hematopoietic stem cell transplantation: prevention and treatment of graft-versus-host disease. Stem Cell Res Ther. 2019; 10:182.
6. Shi Y, Wang Y, Li Q, Liu K, Hou J, Shao C*, et al*. Immunoregulatory mechanisms of mesenchymal stem and stromal cells in inflammatory diseases. Nat Rev Nephrol. 2018; 14:493-507.
7. Jiang XX, Zhang Y, Liu B, Zhang SX, Wu Y, Yu XD*, et al*. Human mesenchymal stem cells inhibit differentiation and function of monocyte-derived dendritic cells. Blood. 2005; 105:4120-4126.
8. Zhu H, Yang F, Tang B, Li XM, Chu YN, Liu YL*, et al*. Mesenchymal stem cells attenuated PLGA-induced inflammatory responses by inhibiting host DC maturation and function. Biomaterials. 2015; 53:688-698.
9. Abumaree MH, Abomaray FM, Alshabibi MA, AlAskar AS, Kalionis B. Immunomodulatory properties of human placental mesenchymal stem/stromal cells. Placenta. 2017; 59:87-95.
10. Dunavin N, Dias A, Li M, McGuirk J. Mesenchymal Stromal Cells: What Is the Mechanism in Acute Graft-Versus-Host Disease? Biomedicines. 2017; 5.
11. Ren G, Zhang L, Zhao X, Xu G, Zhang Y, Roberts AI*, et al*. Mesenchymal stem cell-mediated immunosuppression occurs via concerted action of chemokines and nitric oxide. Cell Stem Cell. 2008; 2:141-150.
12. Li W, Ren G, Huang Y, Su J, Han Y, Li J*, et al*. Mesenchymal stem cells: a double-edged sword in regulating immune responses. Cell Death Differ. 2012; 19:1505-1513.

13. Sudres M, Norol F, Trenado A, Gregoire S, Charlotte F, Levacher B*, et al*. Bone marrow mesenchymal stem cells suppress lymphocyte proliferation in vitro but fail to prevent graft-versus-host disease in mice. J Immunol. 2006; 176:7761-7767.
14. Harrell CR, Jovicic N, Djonov V, Arsenijevic N, Volarevic V. Mesenchymal Stem Cell-Derived Exosomes and Other Extracellular Vesicles as New Remedies in the Therapy of Inflammatory Diseases. Cells. 2019; 8.
15. Wu P, Zhang B, Shi H, Qian H, Xu W. MSC-exosome: A novel cell-free therapy for cutaneous regeneration. Cytotherapy. 2018; 20:291-301.
16. Toh WS, Lai RC, Zhang B, Lim SK. MSC exosome works through a protein-based mechanism of action. Biochem Soc Trans. 2018; 46:843-853.
17. Zhang B, Yin Y, Lai RC, Tan SS, Choo AB, Lim SK. Mesenchymal stem cells secrete immunologically active exosomes. Stem Cells Dev. 2014; 23:1233-1244.
18. Chen W, Huang Y, Han J, Yu L, Li Y, Lu Z*, et al*. Immunomodulatory effects of mesenchymal stromal cells-derived exosome. Immunol Res. 2016; 64:831-840.
19. Thery C, Zitvogel L, Amigorena S. Exosomes: composition, biogenesis and function. Nat Rev Immunol. 2002; 2:569-579.
20. Valadi H, Ekstrom K, Bossios A, Sjostrand M, Lee JJ, Lotvall JO. Exosome-mediated transfer of mRNAs and microRNAs is a novel mechanism of genetic exchange between cells. Nat Cell Biol. 2007; 9:654-659.
21. Zhu Y, Yu J, Yin L, Zhou Y, Sun Z, Jia H*, et al*. MicroRNA-146b, a Sensitive Indicator of Mesenchymal Stem Cell Repair of Acute Renal Injury. Stem Cells Transl Med. 2016; 5:1406-1415.
22. Ti D, Hao H, Tong C, Liu J, Dong L, Zheng J*, et al*. LPS-preconditioned mesenchymal stromal cells modify macrophage polarization for resolution of chronic inflammation via exosome-shuttled let-7b. J Transl Med. 2015; 13:308.
23. Li X, Liu L, Yang J, Yu Y, Chai J, Wang L*, et al*. Exosome Derived From Human Umbilical Cord Mesenchymal Stem Cell Mediates MiR-181c Attenuating Burn-induced Excessive Inflammation. EBioMedicine. 2016; 8:72-82.
24. Ye D, Zhang T, Lou G, Liu Y. Role of miR-223 in the pathophysiology of liver diseases. Exp Mol Med. 2018; 50:128.
25. Zhu H, Guo ZK, Jiang XX, Li H, Wang XY, Yao HY*, et al*. A protocol for isolation and culture of mesenchymal stem cells from mouse compact bone. Nat Protoc. 2010; 5:550-560.
26. Lu LL, Liu YJ, Yang SG, Zhao QJ, Wang X, Gong W*, et al*. Isolation and characterization of human umbilical cord mesenchymal stem cells with hematopoiesis-supportive function and other potentials. Haematologica. 2006; 91:1017-1026.
27. Ying W, Riopel M, Bandyopadhyay G, Dong Y, Birmingham A, Seo JB*, et al*. Adipose Tissue Macrophage-Derived Exosomal miRNAs Can Modulate In Vivo and In Vitro Insulin Sensitivity. Cell. 2017; 171:372-384 e312.

28. Devadas S, Das J, Liu C, Zhang L, Roberts AI, Pan Z*, et al*. Granzyme B is critical for T cell receptor-induced cell death of type 2 helper T cells. Immunity. 2006; 25:237-247.
29. Miao S, Tang B, Liu H, Wang Z, Shi Y, Dong Y*, et al*. CXCR3 blockade combined with cyclosporine A alleviates acute graft-versus-host disease by inhibiting alloreactive donor T cell responses in a murine model. Mol Immunol. 2018; 94:82-90.
30. Fulton LM, Taylor NA, Coghill JM, West ML, Foger N, Bear JE*, et al*. Altered T-cell entry and egress in the absence of Coronin 1A attenuates murine acute graft versus host disease. Eur J Immunol. 2014; 44:1662-1671.
31. Di Trapani M, Bassi G, Midolo M, Gatti A, Kamga PT, Cassaro A*, et al*. Differential and transferable modulatory effects of mesenchymal stromal cell-derived extracellular vesicles on T, B and NK cell functions. Sci Rep. 2016; 6:24120.
32. Liu W, Rong Y, Wang J, Zhou Z, Ge X, Ji C*, et al*. Exosome-shuttled miR-216a-5p from hypoxic preconditioned mesenchymal stem cells repair traumatic spinal cord injury by shifting microglial M1/M2 polarization. J Neuroinflammation. 2020; 17:47.
33. Ranganathan P, Heaphy CE, Costinean S, Stauffer N, Na C, Hamadani M*, et al*. Regulation of acute graft-versus-host disease by microRNA-155. Blood. 2012; 119:4786-4797.
34. Tang B, Li X, Liu Y, Chen X, Li X, Chu Y*, et al*. The Therapeutic Effect of ICAM-1-Overexpressing Mesenchymal Stem Cells on Acute Graft-Versus-Host Disease. Cell Physiol Biochem. 2018; 46:2624-2635.
35. Reiss Y, Hoch G, Deutsch U, Engelhardt B. T cell interaction with ICAM-1-deficient endothelium in vitro: essential role for ICAM-1 and ICAM-2 in transendothelial migration of T cells. Eur J Immunol. 1998; 28:3086-3099.
36. Zitzer NC, Garzon R, Ranganathan P. Toll-Like Receptor Stimulation by MicroRNAs in Acute Graft-vs.-Host Disease. Front Immunol. 2018; 9:2561.

Figures

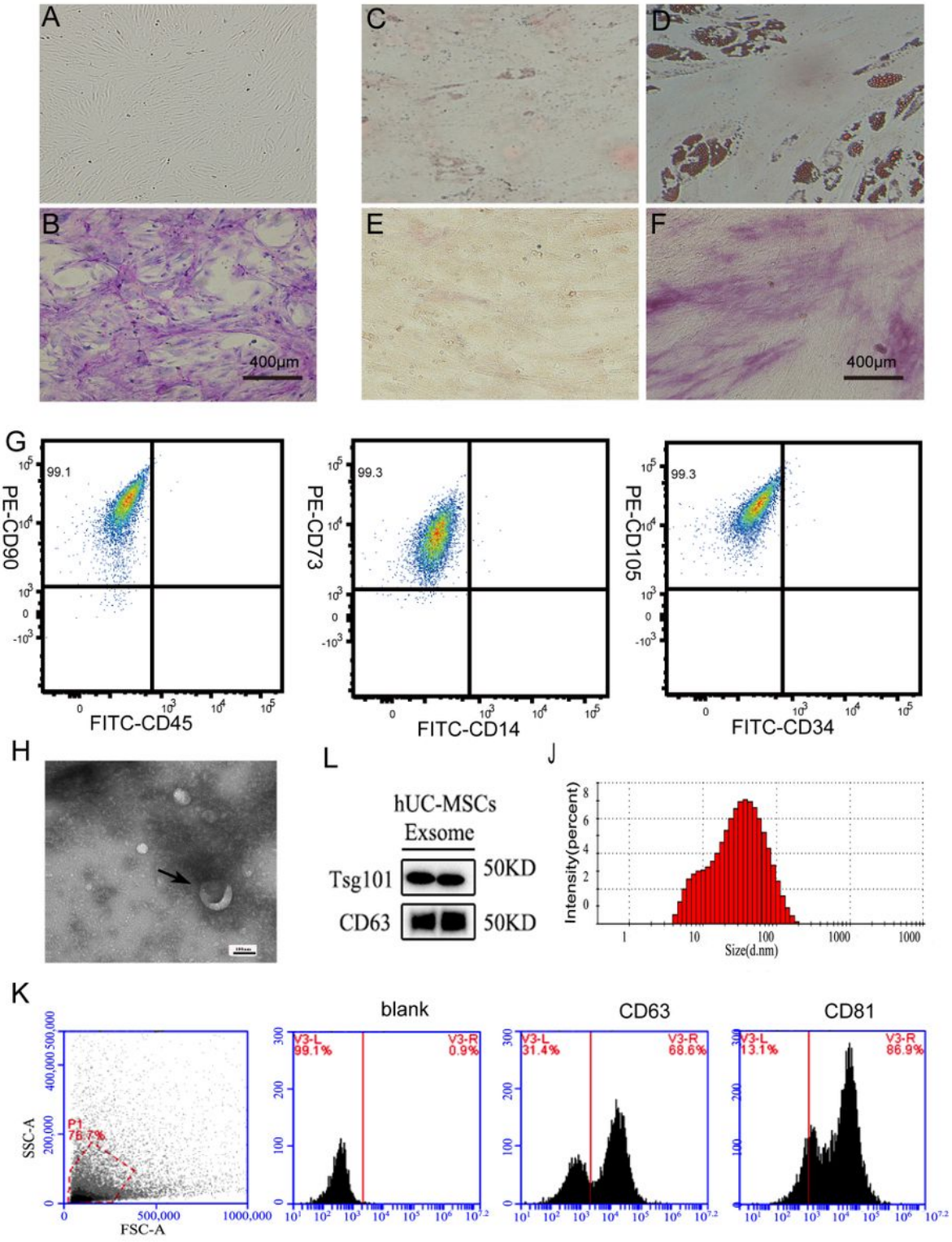

Figure 1

Identification of exosomes derived from human umbilical cord mesenchymal stem cells (huc-MSCs). Nucleated cells isolated from umbilical cord displayed a fibroblast-like morphology (A). The adherent cells (P3) were stained with Wright-Giemsa (B). Adipogenesis differentiation was indicated by the presence of lipid drops that stained with Oil red (C and D; C: control; D: experimental group). Osteogenic differentiation was shown by intracytoplasmic accumulation of alkaline phosphatase (E and F, E: control;

F: experimental group). The phenotype of huc-MSC was detected by flow cytometry. CD45, CD34, and CD14 were negative while CD73, CD105, and CD90 were positive (G). Exosomes secreted by huc-MSCs (marked by the black arrows) were observed under electron microscopy (H). Exosome-specific markers (e.g. TSG101 and CD63) were positive by Western blot analysis (I). NanoSight analysis indicated that particle size of exosome secreted from MSCs was 30–100 nm (J). Analysis of exosome-specific markers CD81 and CD63 was positive by flow cytometry (K)

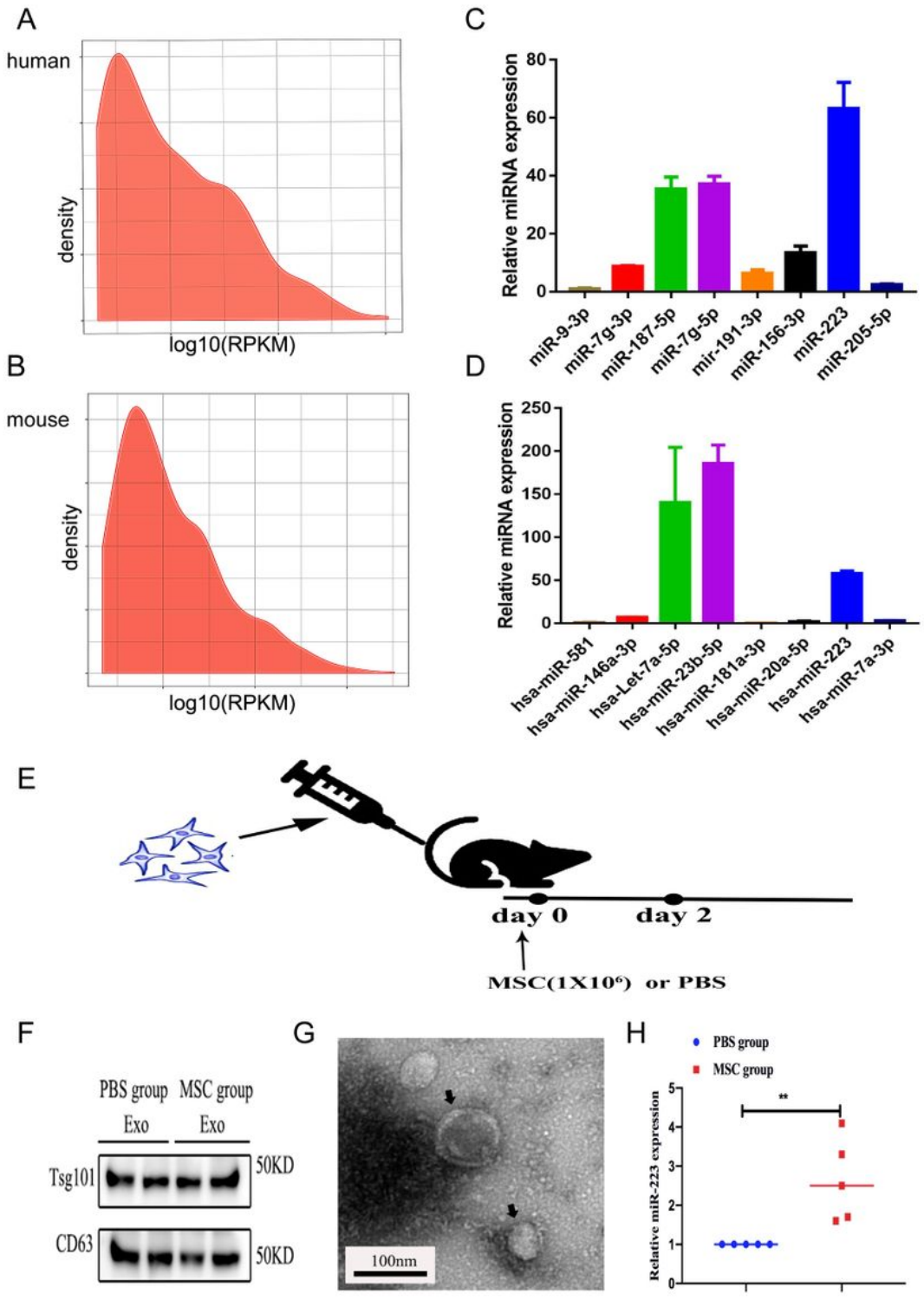

Figure 2

MSCs-derived exosomes contain miR-223 MiRNA expression spectrum in huc-MSCs derived exosomes (A) and mb-MSCs derived exosomes (B) were analyzed by high-throughput sequencing. High expression of miR-223 in huc-MSCs derived exosomes (C) and in mb-MSCs derived exosomes (D) was measured by qPCR. MSC (1×106/dose) was injected into C57BL/6 mice. About 48 hrs after injection, the serum-derived exosomes were isolated, and the expression of miR-223 was tested by qPCR (E). Western blot analysis of serum exosome-specific markers TSG101 and CD63 was positive (F). Exosomes secreted by mb-MSCs (marked by the black arrows) were observed under electron microscopy (G). qPCR indicated the high expression of miR-223 about 48hrs after injection (H). Data were presented as mean ± SEM. n = 5 per group. **P<0.01

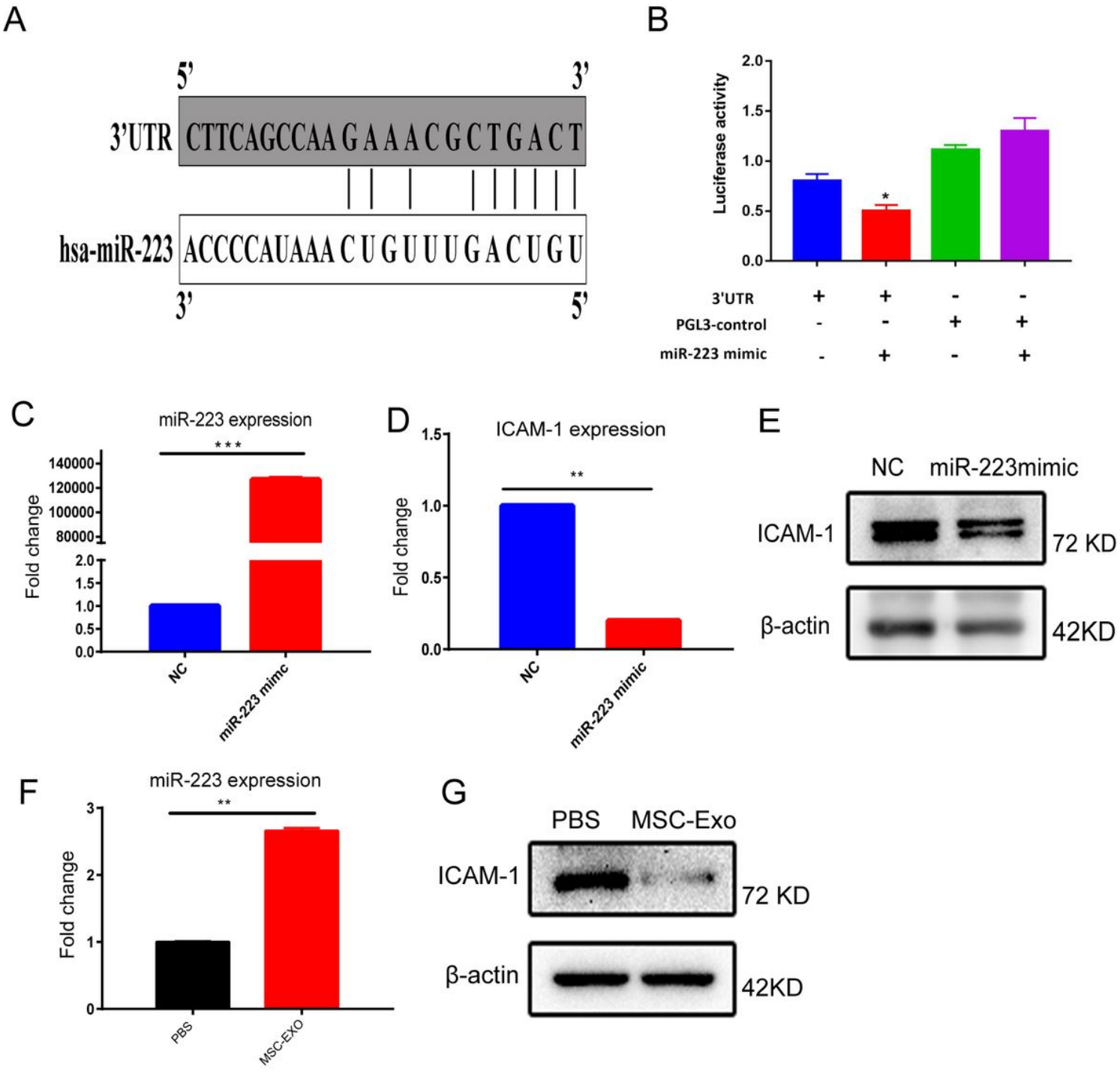

Figure 3

MSC-EV derived miR-223 inhibited ICAM-1 expression Bioinformatic analysis indicated that miR-223 regulated the expression 3'UTR of ICAM-1 (A). Transfection of miR-223 mimic induced significant down-regulation of ICAM-1 (B). High expression of miR-223 by qPCR after transfection of 100nM miR-223 mimics (C). ICAM-1 mRNA and protein expression showed decrease as revealed by qPCR and Western blot (D, E). After 24hr co-culturing of MSC-EV (2 μg) with HUVECs, the expression of ICAM-1 in HUVECs

showed decrease as revealed by qPCR (F) and Western blot (G). Data were presented as mean ± SEM. n = 3 per group. *P<0.05, ***P<0.001

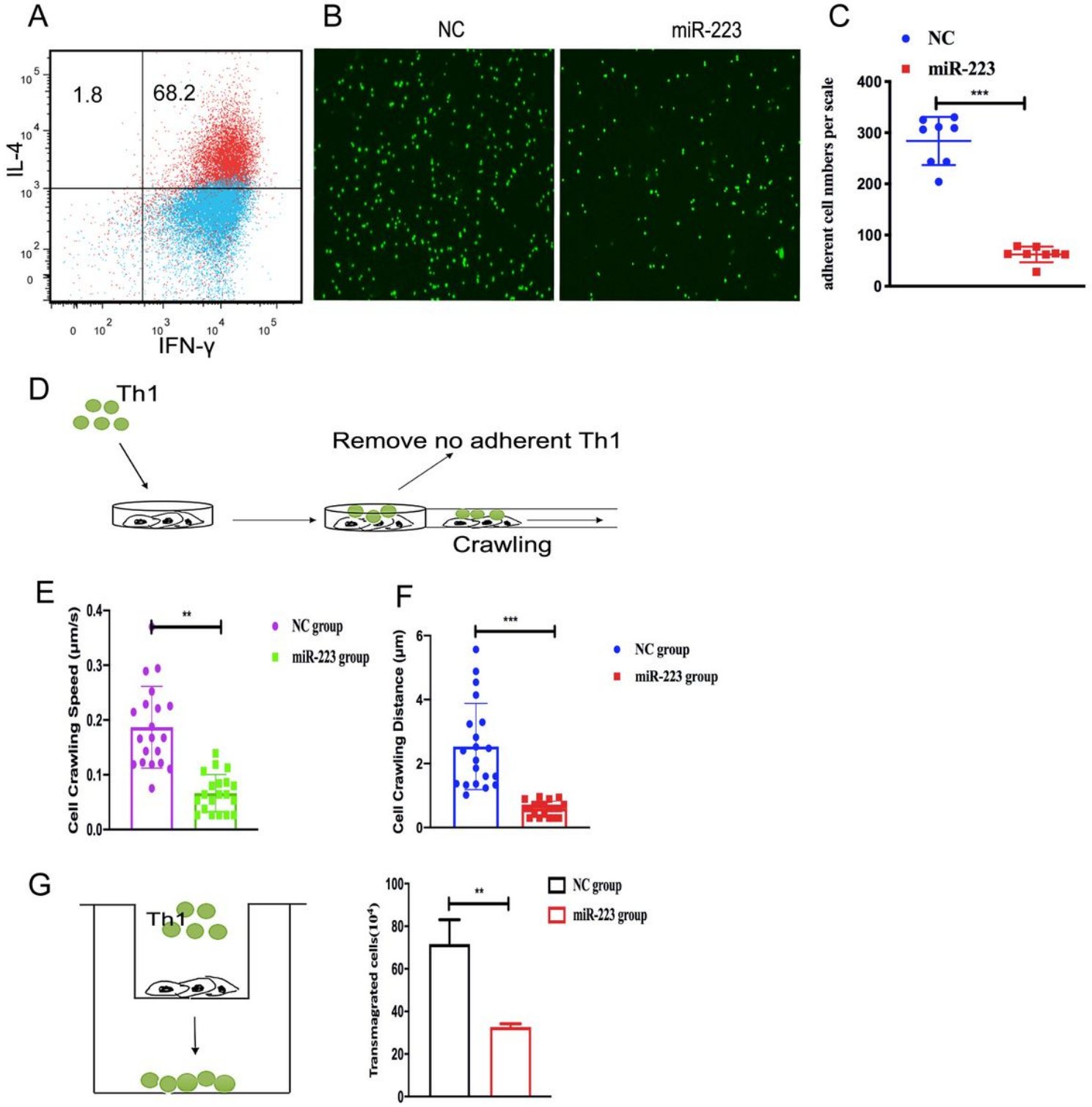

Figure 4

MiR-223 impaired T cell crawling, adhesion and transmigration in vitro. Measurement of CD4+ Th1 differentiation induced with anti-CD3ε (3 μg/ml), anti-CD28 (5 μg/ml), IFN-γ (20 ng/ml), IL-12 (5 ng/ml), and anti-IL4 (5 μg/ml) using flow cytometry (A). Adhesion assay for the Th1 cells stained with green

CellTracker™ and cocultured with mLEC transfected miR-223 mimics (100 nM) or NC for 45 min (B). The average number of green adherent cells in transfected miR-223 group showed significant decrease (C). Crawling assay for the Th1 cells stained with green CellTracker™ seeded on the mLEC transfected miR-223 mimics or NC for 20min. Time-lapse imaging was performed on Operetta CLS™ (D). Compare with NC group, there was significant decrease in the crawling speed and distance of T cells in miR-223 mimics group (E, F). The number of Th1 cells stained with green CellTracker™ in miR-223 group was significantly lower compared with that of normal control (G). Data were presented as mean ± SEM. n = 5 per group. **P<0.01, ***P<0.001

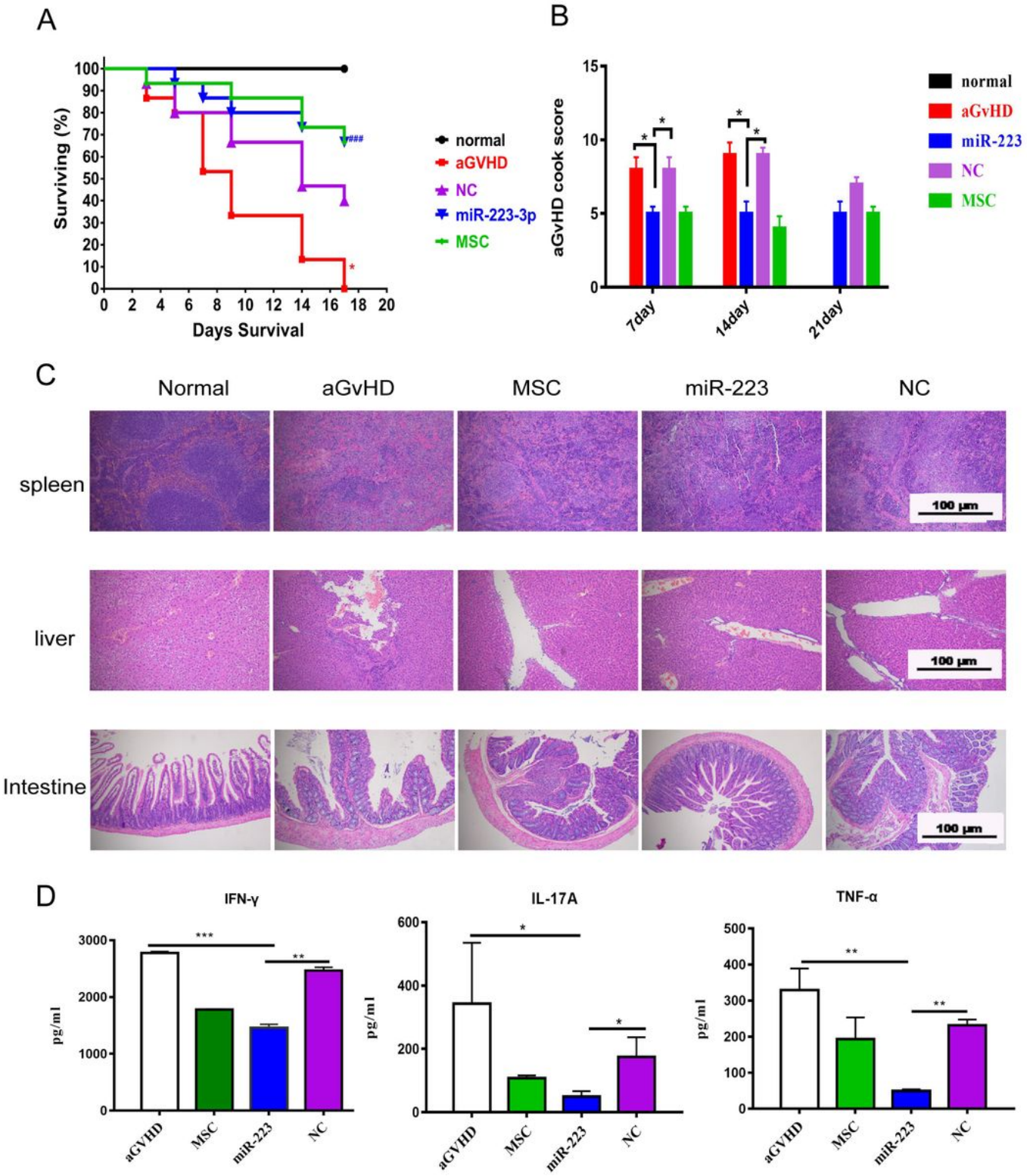

Figure 5

MiR-223 infusion remarkably inhibited the development of aGvHD Recipient BABL/6 mice were irradiated (8.0 Gy) and intravenously injected with C57BL/6 bone marrow cells plus splenocytes. The survival rate of miR-223 group was further improved compared with the other groups (A). The clinical aGvHD scores of miR-223 group of mice were significant alleviated compared with the scores of the aGvHD and NC groups of mice (B). For the representative pathologic changes on day 14, miR-223 infusion dramatically

decreased lymphocyte infiltration in the GvHD target tissues, including the spleen, liver and intestine (C). The inflammatory cytokine level (IFN-γ, IL-17a, and TNF-α) showed significant decline in the blood serum of the miR-223 group compared with that of the aGvHD or NC (D). Data were presented as mean ± SEM. n = 5 per group. *P<0.05, **P<0.01, ***P<0.001.

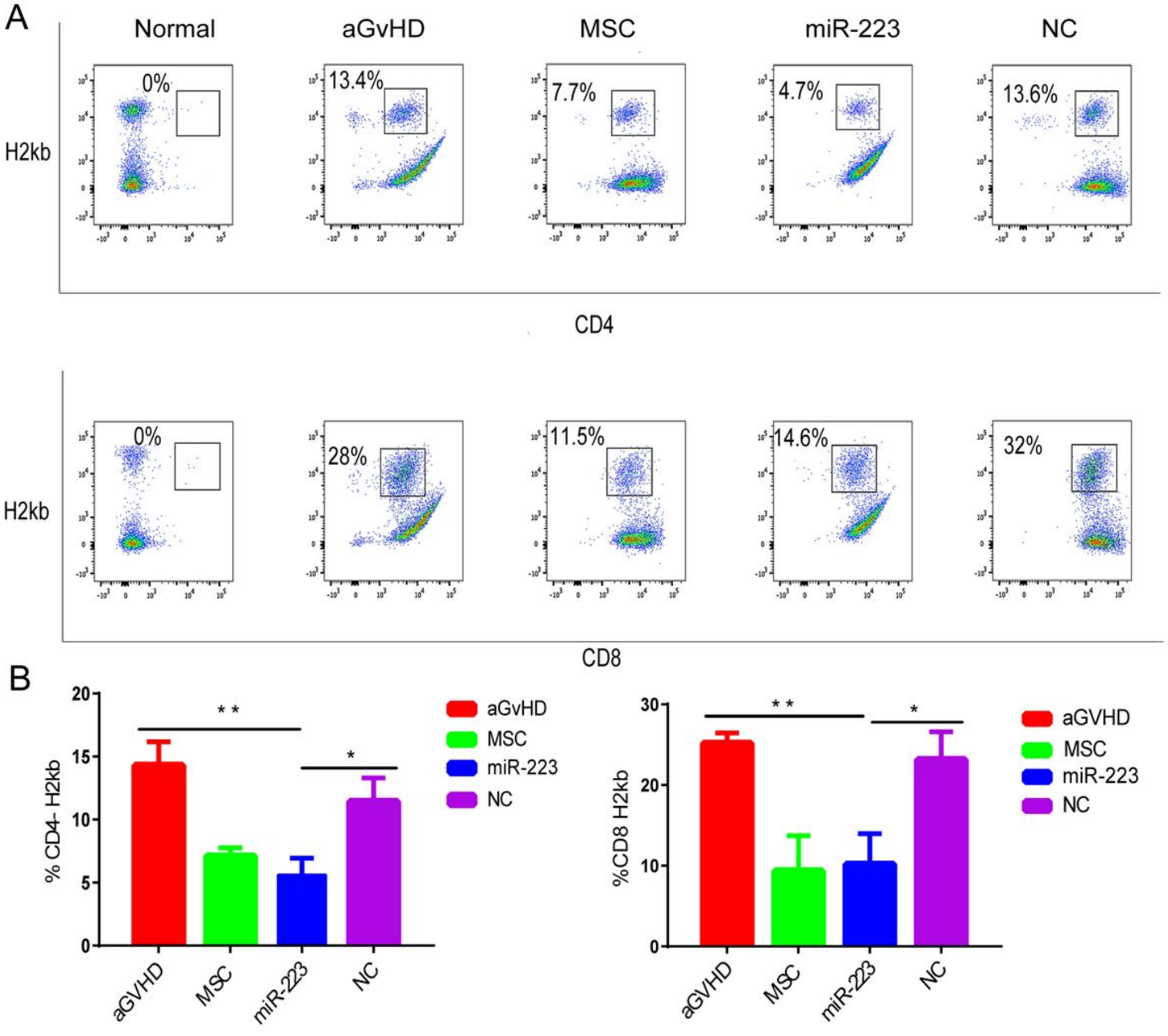

Figure 6

MiR-223 reduced donor T cell migration to recipient mice spleens The proportion of H2kb + CD4 and CD8 T cell in recipient mice spleens on day 7 was assessed by flow cytometry. Compare with NC and aGvHD group, H2kb + CD4 and H2kb + CD8 cell percentages in miR-223 group showed significant reduction (A). The average number of H2kb + CD4 and H2kb + CD8 cells in miR-223 group showed significant decline (B). Data were presented as mean ± SEM. n = 7 per group. *P<0.05, **P<0.01

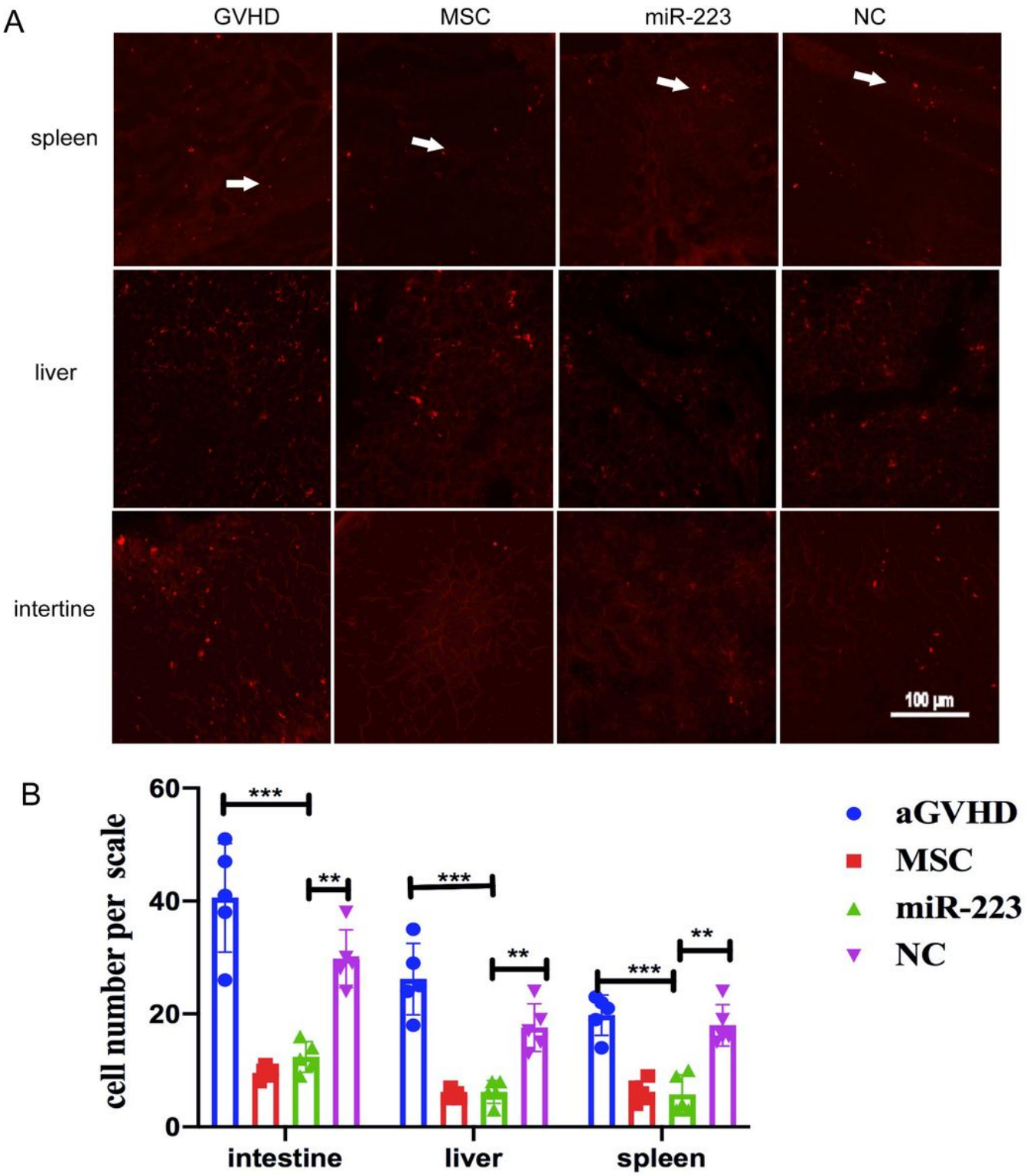

Figure 7

MiR-223 reduced donor T cell homing to recipient tissues and organs. The red CM-dil-labeled splenic T cells and bone marrow cells were transplanted into aGvHD mice. On day 3, the CM-dil-labeled splenic T cells migrated to recipient mice spleen, liver and intestine in vivo. Compared with NC and aGvHD group, significant decline was noticed in the CM-dil-labeled splenic T cells in miR-223 group (A). Compared with NC and aGvHD group, the average number of red CM-dil-labeled cells in spleen, liver or intestine showed

significant decline in miR-223 groups. (B). Five fields were randomly in 5 mice. Data were presented as mean ± SEM. n = 5 per group. *P<0.05, **P<0.01, ***P<0.001.

Supplementary Files

This is a list of supplementary files associated with this preprint. Click to download.

- Supplementaryvideo2TimeMovieline21NC.wmv
- Supplementaryvideo2TimeMovieline21NC.wmv
- Supplementaryvideo1TimeMovieline31miR223.wmv
- Supplementaryvideo1TimeMovieline31miR223.wmv